Space-Time Shift Keying: A Unified MIMO Architecture

S. Sugiura, S. Chen and L. Hanzo

School of ECS, University of Southampton, SO17 1BJ, UK, Tel: +44-23-8059-3125, Fax: +44-23-8059-4508
Email: {ss07r,sqc,lh}@ecs.soton.ac.uk, http://www-mobile.ecs.soton.ac.uk

***Abstract*—In this paper, we propose a novel Space-Time Shift Keying (STSK) modulation scheme for MIMO communication systems, where the concept of spatial modulation is extended to include both the space and time dimensions, in order to provide a general shift-keying framework. More specifically, in the proposed STSK scheme one out of Q dispersion matrices is activated during each transmitted block, which enables us to strike a flexible diversity and multiplexing tradeoff. This is achieved by optimizing both the space-time block duration as well as the number of the dispersion matrices in addition to the number of transmit and receive antennas. We will demonstrate that the resultant equivalent system model does not impose any inter-channel interference, and hence the employment of single-stream maximum likelihood detection becomes realistic at a low-complexity. Furthermore, we propose a Differential STSK (DSTSK) scheme, assisted by the Cayley unitary transform, which does not require any Channel State Information (CSI) at the receiver. Naturally, dispensing with CSI is achieved at the cost of the usual error-doubling in comparison to Coherent STSK (CSTSK). Additionally, we introduce an enhanced CSTSK scheme, which avoids the requirement of inter-antenna synchronization between the RF chains associated with the transmit antenna elements by imposing a certain constraint on the dispersion matrix design.**

I. Introduction

The Vertical Bell Laboratories Layered Space-Time (V-BLAST) [1] scheme is capable of attaining a high multiplexing gain at the cost of a substantial decoding complexity imposed by mitigating the effects of Inter-Channel Interference (ICI). By contrast, Space-Time Block Codes (STBCs) [2] were developed to achieve the maximum attainable diversity order, although the maximum bandwidth efficiency of the full-rate orthogonal STBCs is limited to one bit per symbol duration. Furthermore, Hassibi and Hochwald [3] proposed the unified space-time transmission architecture of Linear Dispersion Codes (LDCs), which subsumes both the V-BLAST and Alamouti's STBC scheme in its ultimate form and it is capable of striking a flexible tradeoff between the achievable diversity and multiplexing gains. Additionally, in [4] the differential-encoding assisted counterpart of LDCs was introduced in order to enable non-coherent detection at the receiver in the absence of Channel State Information (CSI), which was referred to as Differential LDC (DLDC).

Recently, the sophisticated concept of Spatial Modulation (SM) [5], [6] and Space-Shift Keying (SSK) [7] was invented for Multiple-Input Multiple-Output (MIMO) communication systems. The key idea is the activation of one of a total of M antenna elements (AEs) at each symbol duration, leading to an additional means of conveying source information, while removing the effects of ICI. Hence, this arrangement allows the employment of low-complexity single-antenna-based Maximum Likelihood (ML) detection, while V-BLAST requires the potentially excessive-complexity joint detection of multiple antennas' signals. As a result, it was demonstrated in [5]–[7] that SM has the potential of outperforming other MIMO arrangements, such as V-BLAST and Alamouti's STBC schemes.

On the other hand, since SM adopted V-BLAST's high-rate architecture, it has to rely on the employment of multiple DownLink (DL) receive AEs for the sake of combating the effects of fading channels. However, accommodating multiple DL elements imposes challenges, when transmitting to mobiles. Additionally, when aiming for a linear increase in the transmission rate, the number of transmit antennas employed in the context of [5]–[7] has to be increased exponentially. We will circumvent this problem by introducing a new solution. Furthermore, a coherently detected SM scheme requires CSI at the receiver, although it is a challenging task to acquire accurate CSI for high-speed vehicles, which may require a high pilot overhead and imposes a substantial processing complexity. The resultant CSI estimation error is expected to erode the achievable performance.

Against this background the novel contributions of this paper are as follows: Inspired by the SM scheme, we propose the novel concept of Space-Time Shift Keying (STSK) modulation, which constitutes a generalized shift-keying architecture utilizing both the space as well as time dimensions and hence includes the SM and SSK schemes as special cases. More specifically, the STSK scheme is based on the activation of Q number of appropriately indexed space-time dispersion matrices within each STSK block duration, rather than that of the indexed antennas at each symbol duration, as in the SM scheme of [5]–[7]. As a benefit of its high degree of design-freedom, our STSK scheme is capable of striking a flexible diversity versus multiplexing gain tradeoff, which is achieved by optimizing both the number and size of the dispersion matrices as well as the number of transmit and receive antennas. More specifically, our STSK scheme is capable of exploiting both transmit as well as receive diversity gains, unlike the conventional SM and SSK schemes, which can only attain receive diversity gain. Furthermore, since no ICI is imposed by the resultant equivalent system model of the STSK scheme, the employment of single-stream-based ML detection becomes realistic. Additionally, we introduce an improved STSK structure, which enables us to dispense with any symbol-level time-synchronization between the RF chains associated with the transmit AEs, similarly to the SM scheme. As the extension of the above-mentioned Coherent STSK (CSTSK) scheme, we introduce a Differentially-encoded STSK (DSTSK) arrangement, assisted by the Cayley unitary transform based technique of [4], which does not require any CSI estimation at the receiver. More specifically, by employing the Cayley transform in the proposed DSTSK scheme we arrive at a linearized equivalent system model, which is common with that of the CSTSK scheme. Hence the DSTSK scheme retains the fundamental benefits of the CSTSK scheme, although naturally, the corresponding non-coherent receiver suffers from the well-known performance loss compared to its coherent counterpart.

II. Space-Time Shift Keying Modulation

In this contribution we consider an $(M \times N)$-element MIMO system, where M AEs are employed at the transmitter, while the receiver is equipped with N AEs, while assuming a frequency-flat Rayleigh fading environment. In general the block-based system model can be described as

$$\boldsymbol{Y}(i) = \boldsymbol{H}(i)\boldsymbol{S}(i) + \boldsymbol{V}(i), \tag{1}$$

where $\boldsymbol{Y}(i) \in \mathcal{C}^{N\times T}$ represents the received signals and $\boldsymbol{S}(i) \in \mathcal{C}^{M\times T}$ denotes the space-time signals and the mth row's elements are transmitted from the mth antenna, while i indicates the STSK block index. Furthermore, $\boldsymbol{H}(i) \in \mathcal{C}^{N\times M}$ and $\boldsymbol{V}(i) \in \mathcal{C}^{N\times T}$ denote the channel and noise components, each obeying the complex-valued zero-mean Gaussian distribution of $\mathcal{CN}(0,1)$ and of $\mathcal{CN}(0,N_0)$,

The financial support of the EU under the auspices of the Optimix project and of the EPSRC UK is gratefully acknowledged. The work of S. Sugiura was also sponsored in part by the Toyota Central R&D Labs., Inc., Japan.

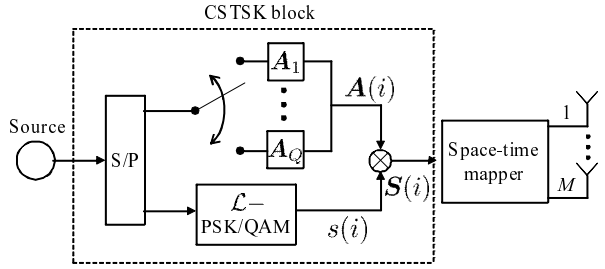

Fig. 1. Transmitter structure of our coherent STSK scheme.

TABLE I
EXAMPLE OF STSK MODULATION SCHEME, MAPPING 3 BITS PER SPACE-TIME BLOCK, WITH THE AID OF L–PSK CONSTELLATION

Input bits	$Q=1$, $\mathcal{L}=8$		$Q=2$, $\mathcal{L}=4$		$Q=4$, $\mathcal{L}=2$		$Q=8$, $\mathcal{L}=1$	
	$\boldsymbol{A}(i)$	$s(i)$	$\boldsymbol{A}(i)$	$s(i)$	$\boldsymbol{A}(i)$	$s(i)$	$\boldsymbol{A}(i)$	$s(i)$
000	$\boldsymbol{A}_1$	1	$\boldsymbol{A}_1$	1	$\boldsymbol{A}_1$	1	$\boldsymbol{A}_1$	1
001	$\boldsymbol{A}_1$	$e^{j\frac{\pi}{4}}$	$\boldsymbol{A}_1$	$e^{j\frac{\pi}{2}}$	$\boldsymbol{A}_1$	$e^{j\pi}$	$\boldsymbol{A}_2$	1
010	$\boldsymbol{A}_1$	$e^{j\frac{2\pi}{4}}$	$\boldsymbol{A}_1$	$e^{j\frac{2\pi}{2}}$	$\boldsymbol{A}_2$	1	$\boldsymbol{A}_3$	1
011	$\boldsymbol{A}_1$	$e^{j\frac{3\pi}{4}}$	$\boldsymbol{A}_1$	$e^{j\frac{3\pi}{2}}$	$\boldsymbol{A}_2$	$e^{j\pi}$	$\boldsymbol{A}_4$	1
100	$\boldsymbol{A}_1$	$e^{j\frac{4\pi}{4}}$	$\boldsymbol{A}_2$	1	$\boldsymbol{A}_3$	1	$\boldsymbol{A}_5$	1
101	$\boldsymbol{A}_1$	$e^{j\frac{5\pi}{4}}$	$\boldsymbol{A}_2$	$e^{j\frac{\pi}{2}}$	$\boldsymbol{A}_3$	$e^{j\pi}$	$\boldsymbol{A}_6$	1
110	$\boldsymbol{A}_1$	$e^{j\frac{6\pi}{4}}$	$\boldsymbol{A}_2$	$e^{j\frac{2\pi}{2}}$	$\boldsymbol{A}_4$	1	$\boldsymbol{A}_7$	1
111	$\boldsymbol{A}_1$	$e^{j\frac{7\pi}{4}}$	$\boldsymbol{A}_2$	$e^{j\frac{3\pi}{2}}$	$\boldsymbol{A}_4$	$e^{j\pi}$	$\boldsymbol{A}_8$	1

respectively, where N_0 represents the noise variance.

A. Coherent STSK scheme

Fig. 1 depicts the transmitter structure of our CSTSK scheme, where Q dispersion matrices $\boldsymbol{A}_q \in \mathcal{C}^{M\times T}$ $(q=1,\cdots,Q)$ are pre-assigned in advance of any transmission. A total of $\log_2(Q\cdot\mathcal{L})$ source bits are mapped to each space-time block $\boldsymbol{S}(i) \in \mathcal{C}^{M\times T}$ by the CSTSK scheme of Fig. 1, yielding

$$\boldsymbol{S}(i) = s(i)\boldsymbol{A}(i), \tag{2}$$

where $s(i)$ is the complex-valued symbol of the conventional modulation scheme employed, such as $\mathcal{L}$-PSK or $\mathcal{L}$-QAM, which is associated with $\log_2\mathcal{L}$ number of input bits. By contrast, the specific matrix $\boldsymbol{A}(i)$ is selected from the Q dispersion matrices $\boldsymbol{A}_q$ $(q=1,\cdots,Q)$ according to $\log_2 Q$ number of input bits. In this way, an additional means of transmitting further information bits was created. To be specific, we exemplify in Table I the mapping rule of our CSTSK modulation scheme, where a fixed number of $\log_2(Q\cdot\mathcal{L})=3$ bits per space-time block $\boldsymbol{S}(i)$ are transmitted by employing $\mathcal{L}$–PSK, for the specific cases of $(Q,\mathcal{L})$ =$(1,8;2,4;4,2;8,1)$. As seen from Table I, there are several possible combinations of the number of dispersion matrices Q and of the constellation size $\mathcal{L}$, given 3 source bits per space-time block. Moreover, the normalized throughput per time-slot (or per symbol) R of our STSK scheme may be expressed as $R=\log_2(Q\cdot\mathcal{L})/T$ bits/symbol.

Having generated the space-time block $\boldsymbol{S}(i)$ to be transmitted, we then introduce the ML detection algorithm of our CSTSK scheme. By applying the vectorial stacking operation $vec()$ to the received signal block $\boldsymbol{Y}(i)$ in Eq. (1), we arrive at the linearized equivalent system model formulated as follows: [8]

$$\bar{\boldsymbol{Y}}(i) = \bar{\boldsymbol{H}}(i)\chi\boldsymbol{K}(i) + \bar{\boldsymbol{V}}(i), \tag{3}$$

with the relations of

$$\bar{\boldsymbol{Y}}(i) = vec(\boldsymbol{Y}(i)) \quad \in \mathcal{C}^{NT\times 1}, \tag{4}$$
$$\bar{\boldsymbol{H}}(i) = \boldsymbol{I}\otimes\boldsymbol{H}(i) \quad \in \mathcal{C}^{NT\times MT}, \tag{5}$$
$$\bar{\boldsymbol{V}}(i) = vec(\boldsymbol{V}(i)) \quad \in \mathcal{C}^{NT\times 1}, \tag{6}$$
$$\chi \quad = [vec(\boldsymbol{A}_1)\cdots vec(\boldsymbol{A}_Q)] \in \mathcal{C}^{MT\times Q}, \tag{7}$$

where $\boldsymbol{I}$ is the identity matrix and $\otimes$ is the Kronecker product. Furthermore, the equivalent transmitted signal vector $\boldsymbol{K}(i)\in\mathcal{C}^{Q\times 1}$ is written as

$$\boldsymbol{K}(i) = [\underbrace{0,\cdots,0}_{q-1}, s(i), \underbrace{0,\cdots,0}_{Q-q}]^T, \tag{8}$$

where the modulated symbol $s(i)$ is situated in the qth element, noting that the index q corresponds to the index of the dispersion matrix $\boldsymbol{A}_q$ activated during the ith STSK block. Therefore, the number of legitimate transmit signal vectors $\boldsymbol{K}$ is given by $Q\cdot\mathcal{L}$. Additionally, in order to maintain a unity average transmission power for each STSK symbol duration, each of the Q dispersion matrices has to obey the power constraint of $\mathrm{tr}[\boldsymbol{A}_q^H\boldsymbol{A}_q]=T$ $(q=1,\cdots,Q)$, where $\mathrm{tr}[\cdot]$ indicates the trace operation. Our design rule used for generating the dispersion matrices $\boldsymbol{A}_q$ will be described in Section IV.

Since the equivalent system model of Eq. (3) is free from the effects of ICI, we can employ the single-stream-based ML detector of [6], which imposes a low complexity. Let us consider that (q,l) correspond to the specific input bits of a STSK block, which are mapped to the lth $(l=1,\cdots,\mathcal{L})$ PSK symbol and qth $(q=1,\cdots,Q)$ dispersion matrix. Then the estimates $(\hat{q},\hat{l})$ are given by

$$(\hat{q},\hat{l}) = \arg\min_{q,l} ||\bar{\boldsymbol{Y}}(i) - \bar{\boldsymbol{H}}(i)\chi\boldsymbol{K}_{q,l}||^2 \tag{9}$$
$$= \arg\min_{q,l} ||\bar{\boldsymbol{Y}}(i) - s_l\left(\bar{\boldsymbol{H}}(i)\chi\right)_q||^2, \tag{10}$$

where s_l represents the lth symbol in the $\mathcal{L}$-point constellation and the signal vector $\boldsymbol{K}_{q,l}\in K$ $(1\le q\le Q,\ 1\le l\le\mathcal{L})$ indicates

$$\boldsymbol{K}_{q,l} = [\underbrace{0,\cdots,0}_{q-1}, s_l, \underbrace{0,\cdots,0}_{Q-q}]^T. \tag{11}$$

Furthermore, $\left(\bar{\boldsymbol{H}}(i)\chi\right)_q$ is the qth column vector of the matrix $\bar{\boldsymbol{H}}(i)\chi$. As mentioned in [6], this low-complexity ML detector exhibits the optimal detection performance in the uncoded scenario, where no *a priori* information is provided and the source bits are equi-probable. In the rest of this paper, we employ the parameter-based notation of our CSTSK scheme formulated as CSTSK(M,N,T,Q) for ease of treatment.

To elaborate a little further, our CSTSK scheme includes the SM arrangement as its special case. To be specific, the CSTSK$(M,N,1,Q=M)$ scheme having the dispersion matrices of $\boldsymbol{A}_1=[1\ 0,\cdots,0]^T, \boldsymbol{A}_2=[0\ 1\ 0,\cdots,0]^T,\cdots,\boldsymbol{A}_Q=[0,\cdots,0\ 1]^T$ exhibits a system structure, which is identical to that of the SM scheme employing (M,N) transmit and receive antennas, noting that in this case χ becomes the identity matrix $\boldsymbol{I}$.

It should also be noted that while SM has to exponentially increase the number of transmit AEs for the sake of linearly increasing the number of transmitted input bits, our CSTSK scheme may circumvent this problem by increasing the number of dispersion matrices Q. Therefore, given an affordable tradeoff in terms of number of transmit antennas M, our CSTSK scheme is capable of optimizing the derived transmission rate and diversity order in a more flexible and efficient manner by appropriately choosing T and Q.

B. Asynchronous CSTSK scheme

As mentioned in [5]–[7], the SM and SSK schemes do not require any symbol-level time synchronization between the transmit antenna circuits, because a single antenna is activated at each symbol instant in these schemes. By contrast, our CSTSK scheme potentially requires IAS for the CSTSK's dispersion matrix activation, which replaces the antenna activation. However, by carefully designing the dispersion matrices $\boldsymbol{A}_q$ $(q=1,\cdots,Q)$ of our CSTSK, we will contrive an Asynchronous CSTSK (A-CSTSK) arrangement dispensing

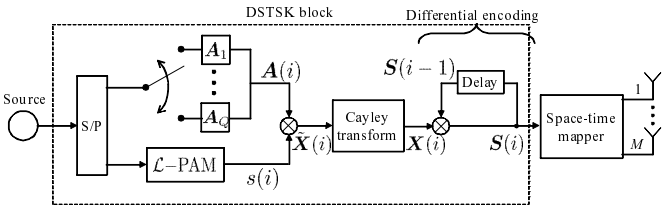

Fig. 2. Transmitter structure of our DSTSK scheme.

with any IAS. More specifically, the structure of each dispersion matrix $\boldsymbol{A}_q$ is constructed so that there is a single non-zero element for each column of the dispersion matrix $\boldsymbol{A}_q$. This constraint enables us to avoid any simultaneous transmission by multiple antennas, similarly to the conventional SM and SSK schemes, while retaining all the benefits of our CSTSK scheme.

C. Differential STSK scheme

The above-mentioned CSTSK scheme and the conventional SM scheme are both based on the *prior* knowledge of CSI and hence the performance degradation imposed by CSI estimation errors is unavoidable. To avoid this limitation, we contrived the corresponding DSTSK scheme as the extension of the CSTSK scheme with the aid of the Cayley unitary transform proposed in [4] and detailed in Section 8.4 of [8].

Fig. 2 shows the transmitter structure of our DSTSK scheme, where Q Hermitian matrices $\boldsymbol{A}_q$ $(q = 1, 2, \cdots, Q)$ are pre-allocated as the dispersion matrices prior to transmissions and $\mathcal{L}$-level Pulse Amplitude Modulation (PAM) is employed. Similarly to the CSTSK scheme of Fig. 1 and detailed in Section II-A, each space-time block contains $\log_2(Q \cdot \mathcal{L})$ source bits, where $\log_2 Q$ bits are mapped to $\boldsymbol{A}(i)$ using the previously outlined process of dispersion-matrix activation, while $\log_2 \mathcal{L}$ bits are mapped to the $\mathcal{L}$-PAM symbols $s(i)$. Thus, analogously to Eq. (2), the Hermitian matrix $\boldsymbol{X}(i) \in \mathcal{C}^{M\times T}$ is calculated as

$$\tilde{\boldsymbol{X}}(i) = s(i)\boldsymbol{A}(i), \tag{12}$$

where we have the relation of $M = T$. Furthermore, based on the Cayley unitary transform technique of [4], the Hermitian matrix $\tilde{\boldsymbol{X}}(i)$ is transformed to the unitary matrix $\boldsymbol{X}(i)$ as follows:[1]

$$\boldsymbol{X}(i) = [\boldsymbol{I} - j\tilde{\boldsymbol{X}}(i)][\boldsymbol{I} + j\tilde{\boldsymbol{X}}(i)]^{-1}, \tag{13}$$

where $\boldsymbol{I}$ is the identity matrix. Finally, the space-time matrix $\boldsymbol{S}(i)$ is differentially-encoded as follows: $\boldsymbol{S}(i) = \boldsymbol{S}(i-1) \cdot \boldsymbol{X}(i)$, where the symbols in the mth row of $\boldsymbol{S}(i)$ are transmitted from the mth transmit AE over T symbol durations.

Assuming that the fading channel envelope remains constant over the two DSTSK block durations $2T$, the corresponding received signal block $\boldsymbol{Y}(i)$ of Eq. (1) is modified to

$$\boldsymbol{Y}(i) = \boldsymbol{Y}(i-1)\boldsymbol{X}(i) + \boldsymbol{V}(i) - \boldsymbol{V}(i-1)\boldsymbol{X}(i), \tag{14}$$

which does not include any channel components. Instead of directly applying optimum ML detection to the received signal of Eq. (14), we introduce the linearization technique of [4] for the sake of facilitating the employment of the ML detector of Eq. (10). More specifically, upon multiplying both sides of Eq. (14) by $[\boldsymbol{I} + j\tilde{\boldsymbol{X}}(i)]$, we arrive at

[1]We note that the Cayley unitary transform of Eq. (13) uniquely connects the unitary matrix $\boldsymbol{X}(i)$ with the Hermitian matrix $\tilde{\boldsymbol{X}}(i)$, therefore enabling the differential unitary encoding and leading to the linearized equivalent system model of Eq. (16). Furthermore, in order to ensure $\tilde{\boldsymbol{X}}(i)$ remains a Hermitian matrix, the modulated symbol $s(i)$ of Eq. (12) has to be a real-valued, rather than a complex-valued symbol, such as PSK and QAM. For this reason, we adopt a PAM constellation in our DSTSK scheme.

TABLE II
COMPUTATIONAL COMPLEXITY REQUIRED FOR THE ML DETECTION OF OUR COHERENT AND DIFFERENTIAL STSK SCHEMES

	Complexity	
CSTSK	$NTQ(4MT + 6\mathcal{L})/\log_2(Q \cdot \mathcal{L})$	(fast fading)
	$NTQ[(4MT + 4\mathcal{L})/\tau + 2\mathcal{L}]/\log_2(Q \cdot \mathcal{L})$	(slow fading)
DSTSK	$NTQ(4MT + 6\mathcal{L})/\log_2(Q \cdot \mathcal{L})$	
SM	$6MN\mathcal{L}/\log_2(M \cdot \mathcal{L})$	(fast fading)
	$(4/\tau + 2)MN\mathcal{L}/\log_2(M \cdot \mathcal{L})$	(slow fading)

$$\underbrace{\boldsymbol{Y}(i) - \boldsymbol{Y}(i-1)}_{\hat{\boldsymbol{Y}}(i)} = \underbrace{-j[\boldsymbol{Y}(i) + \boldsymbol{Y}(i-1)]}_{\hat{\boldsymbol{H}}(i)}\tilde{\boldsymbol{X}}(i) + \underbrace{\{-\boldsymbol{V}(i)[\boldsymbol{I} + j\tilde{\boldsymbol{X}}(i)] - \boldsymbol{V}(i-1)[\boldsymbol{I} - j\tilde{\boldsymbol{X}}(i)]\}}_{\hat{\boldsymbol{V}}(i)}, \tag{15}$$

where $\hat{\boldsymbol{Y}}(i)$ and $\hat{\boldsymbol{H}}(i)$ represent the equivalent received signals and the equivalent channel matrix, while the equivalent noise matrix $\hat{\boldsymbol{V}}(i)$ has independent columns with a covariance of $\hat{N}_0 = N_0(\boldsymbol{I} + \tilde{\boldsymbol{X}}^2)$. Finally, by applying the $vec(\ )$ operation to Eq. (15), we arrive at [4]

$$\bar{\boldsymbol{Y}}(i) = \bar{\boldsymbol{H}}(i)\chi\boldsymbol{K}(i) + \bar{\boldsymbol{V}}(i), \tag{16}$$

where we have $\bar{\boldsymbol{Y}}(i) = vec[\hat{\boldsymbol{Y}}(i)] \in \mathcal{C}^{NT\times 1}$, $\bar{\boldsymbol{H}}(i) = \boldsymbol{I} \otimes \hat{\boldsymbol{H}}(i) \in \mathcal{C}^{NT\times MT}$ and $\bar{\boldsymbol{V}}(i) = vec[\hat{\boldsymbol{V}}(i)] \in \mathcal{C}^{NT\times 1}$, while χ and $\boldsymbol{K}(i)$ are given by Eqs. (7) and (8), respectively, in the same manner as the CSTSK scheme of Section II-A.

Clearly, since the linearized system model of our DSTSK scheme (Eq. (16)) exhibits the same structure as for that of its CSTSK counterpart (Eq. (3)), we can readily invoke the single-stream-based ML detector according to the criterion of Eq. (10), acknowledging that the resultant DSTSK's performance would inevitably suffer from the usual differential encoding induced SNR loss owing to the enhanced noise variance of $\hat{N}_0$.

D. Computational Complexity

Let us now characterize the computational complexity imposed by the ML detection of our CSTSK and DSTSK schemes. Table II lists their complexity, evaluated in terms of the number of real-valued multiplications, noting that a single complex-valued multiplication was considered equivalent to four real-valued multiplications. For reference, the complexity of the SM scheme was also shown in Table II. Furthermore, τ represents an integer, quantifying the coherence block interval in slow fading environments. As seen in Table II, although the SM scheme typically imposes a lower complexity than those of our CSTSK and DSTSK schemes, both the proposed schemes have a substantially lower complexity ML receiver in comparison to classic MIMO schemes, such as V-BLAST, LDCs and DLDCs, which is an explicit benefit of our ICI-free system model.

To be more specific, for the case of fast fading environments, the ML detector of our CSTSK scheme is required to calculate $\bar{\boldsymbol{H}}(i)\chi\boldsymbol{K}_{q,l}$ $(1 \le q \le Q, 1 \le l \le \mathcal{L})$ for each CSTSK block, corresponding to the complexity of $NTQ(4MT + 4\mathcal{L})/\log_2(Q \cdot \mathcal{L})$ in Table II. On the other hand, in slow fading environments, this complexity is reduced to $NTQ(4MT+4\mathcal{L})/[\tau \log_2(Q\cdot\mathcal{L})]$, since the associated calculation can be reused during the channels' coherence time.

For our DSTSK scheme, the equivalent channels $\bar{\boldsymbol{H}}(i)\chi$ have to be calculated for each DSTSK block, regardless of the value τ, as required by the implementation of differential decoding. However, it is worth mentioning that since our DSTSK scheme does not impose a pilot overhead and eliminates the complexity associated with CSI estimation, hence its complexity may be significantly lower than those

of the CSTSK and SM schemes, especially when the corresponding MIMO channels change rapidly.

E. Maximum Achievable Diversity Order of CSTSK

For the general CSTSK block-based system model of Eq. (1), an upper bound of the average probability misinterpreting the transmitted space-time matrix $\boldsymbol{S}$ as $\boldsymbol{S}'$ is given by the Chernoff upper bound as follows:

$$P(\boldsymbol{S} \to \boldsymbol{S}') \leq \frac{1}{\left|\boldsymbol{I}_{M\cdot N} + \frac{1}{4N_0}\boldsymbol{R} \otimes \boldsymbol{I}_N\right|}, \tag{17}$$

where we have $\boldsymbol{R} = (\boldsymbol{S} - \boldsymbol{S}')(\boldsymbol{S} - \boldsymbol{S}')^H$. Furthermore, for high SNRs, Eq. (17) may be simplified to [8]

$$P(\boldsymbol{S} \to \boldsymbol{S}') \leq \frac{1}{[1/(4N_0)]^{m'N} \prod_{i=1}^{m'} \lambda_n^N}, \tag{18}$$

where m' and λ_n are the rank and the nth eigenvalue of $\boldsymbol{R}$, respectively. Let us now define the STC's diversity order as the exponent of its erroneous decision probability curve in Eq. (18). Then the resultant diversity order is determined by the smallest value of the product $m'N$ in Eq. (18). Therefore, we may surmise that the maximum achievable diversity order of our CSTSK scheme is given by $N \cdot \min(M, T)$, where $\min(M, T)$ corresponds to the achievable transmit diversity gain.

III. Capacity of Our CSTSK Scheme

In this section, we characterize the Discrete-input Continuous-output Memoryless Channel (DCMC) capacity [8] of the CSTSK scheme, which is defined for MIMO channels in combination with the specific multi-dimensional signaling set employed. Note that in contrast to the DCMC capacity, Shannon's channel capacity was defined for Continuous-input Continuous-output Memoryless Channels (CCMC) [8], assuming continuous-amplitude discrete-time Gaussian-distributed transmitted signals, where only the transmit power and the bandwidth are restricted.

According to [8], the DCMC capacity of our CSTSK scheme using $\mathcal{L}-$PSK or $\mathcal{L}-$QAM signaling may be expressed as

$$C = \frac{1}{T} \max_{p(\boldsymbol{K}_{1,1}),\cdots,p(\boldsymbol{K}_{Q,\mathcal{L}})} \sum_{q,l} \int_{-\infty}^{\infty} \cdots \int_{-\infty}^{\infty} p(\bar{\boldsymbol{Y}}|\boldsymbol{K}_{q,l}) p(\boldsymbol{K}_{q,l}) \cdot \log_2 \left[\frac{p(\bar{\boldsymbol{Y}}|\boldsymbol{K}_{q,l})}{\sum_{q',l'} p(\bar{\boldsymbol{Y}}|\boldsymbol{K}_{q',l'}) p(\boldsymbol{K}_{q',l'})} \right] d\bar{\boldsymbol{Y}} \text{ (bits/symbol)}. \tag{19}$$

Since Eq. (19) is maximized under the assumption that all the signals $\boldsymbol{K}_{q,l}$ are equi-probable, when we have $p(\boldsymbol{K}_{1,1}) = \cdots = p(\boldsymbol{K}_{Q,\mathcal{L}}) = 1/(Q \cdot \mathcal{L})$, Eq. (19) is simplified to [8]

$$C = \frac{1}{T} \left(\log_2(Q \cdot \mathcal{L}) - \frac{1}{Q \cdot \mathcal{L}} \times \sum_{q,l} E \left[\log_2 \left\{ \sum_{q',l'} \exp(\Psi_{q,l}^{q',l'}) \middle| \boldsymbol{K}_{q',l'} \right\} \right] \right), \tag{20}$$

where we have $\Psi_{q,l}^{q',l'} = -||\bar{\boldsymbol{H}}\chi(\boldsymbol{K}_{q,l} - \boldsymbol{K}_{q',l'}) + \bar{\boldsymbol{V}}||^2 + ||\bar{\boldsymbol{V}}||^2$.

IV. Dispersion Matrix Design Criterion

In our CSTSK and DSTSK schemes the specific design of the dispersion matrices $\boldsymbol{A}_q$ $(q = 1, \cdots, Q)$ significantly affects the achievable performance, similarly to those of LDC and DLDC schemes. More specifically, the dispersion matrices optimized for the LDC and DLDC schemes in [8] for example do not provide our CSTSK and DSTSK schemes with a high performance owing to their different system models. For our CSTSK scheme, the maximization of the DCMC capacity presented in Section III is adopted as the design criterion of the dispersion matrices $\boldsymbol{A}_q$, for the sake of maximizing the achievable capacity, given the constellation size $\mathcal{L}$ as well as the CSTSK parameters of (M, N, T, Q). An random search was implemented under the power constraint.

It was noted in the context of DLDCs [8] that the optimization of the DSTSK's dispersion matrix set $\boldsymbol{A}_q$ for maximizing the capacity is challenging and may lead to non-unique solutions. Therefore, we employ the well-known rank and determinant criterion of [8] for designing the dispersion matrix set $\boldsymbol{A}_q$ of our DSTSK scheme.

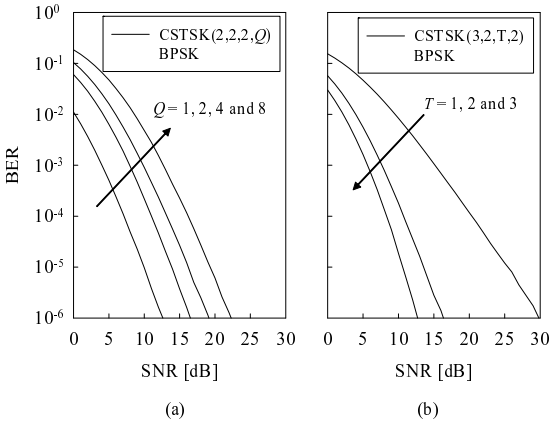

Fig. 3. Achievable BER curves of our CSTSK system, comparing the effects of (a) the number of dispersion matrices Q and (b) the space-time block duration T.

V. Performance Results

In this section we provide our performance results for characterizing both the uncoded and three-stage concatenated STSK schemes. Here, we assumed transmissions over Rayleigh block fading channels having a coherence time of T for our CSTSK scheme, which had a constant envelope over a CSTSK symbol, but faded independently between consecutive CSTSK blocks. By contrast, twice the coherence time of $2T$ was assumed for our DSTSK scheme.

Figs. 3(a) and 3(b) characterize the achievable BER performance of our CSTSK system, comparing the effects of the number of dispersion matrices Q and of the space-time block duration T, respectively. Observe in Fig. 3(a) that upon increasing the value Q in our BPSK-modulated CSTSK$(2, 2, 2, Q)$ scheme from $Q = 1$ to $Q = 4$, the corresponding throughput increased from $R = 0.5$ bits/symbol to $R = 2.0$ bits/symbol, at the expense of a degraded BER performance, while maintaining a diversity order of four. Furthermore, it can be seen in Fig. 3(b) that the diversity order of our BPSK-modulated CSTSK$(3, 2, T, 2)$ arrangement increases upon increasing the space-time block duration T, at the cost of a throughput reduction from $R = 2.0$ bits/symbol to $R = 0.67$ bits/symbol.

Fig. 4 compares the achievable BER performance of our CSTSK$(M, 2, 2, 4)$ scheme and that of the corresponding SM scheme, where the employment of the optimum ML detector of [6] was assumed for the SM scheme. Here, we simulated two scenarios, where the first one considered the normalized throughput of $R = 2.0$ bits/symbol and $(M, N) = (2, 2)$ AEs, while the second one assumed $R = 3.0$ bits/symbol and $(M, N) = (4, 2)$. It was found that our CSTSK scheme outperformed the SM scheme in both the scenarios, while achieving a diversity order of four, as a benefit of exploiting both the achievable transmit and receive diversity gains, while the SM scheme attained only a receive diversity order of two.

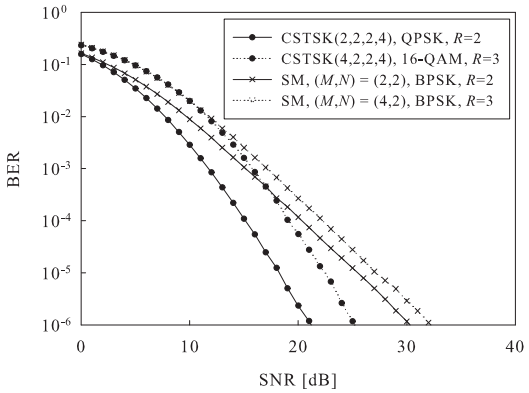

Fig. 4. Achievable BER curves of our CSTSK scheme and the SM scheme, for the cases of the employment of (M, N)=$(2, 2)$ antennas and of (M, N)=$(4, 2)$ antennas.

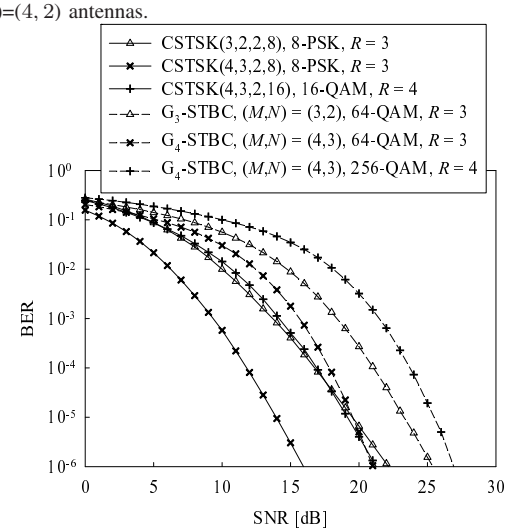

Fig. 5. Achievable BER curves of the diverse CSTSK schemes, compared with the orthogonal STBC schemes. Here, the classic G_3 and G_4 codes [2] were employed as the benchmarkers.

Furthermore, in Fig. 5 we compared the diverse CSTSK schemes with orthogonal STBCs, having the corresponding transmission rate R as well as the same number of transmit and receive antennas (M, N), such as $(M, N) = (3, 2)$ and $(M, N) = (4, 3)$. More specifically, we considered four different CSTSK arrangements, which are given by the 8-PSK modulated CSTSK$(3, 2, 2, 8)$, the 8-PSK modulated CSTSK$(4, 3, 2, 8)$ and the 16-QAM CSTSK$(4, 3, 2, 16)$. Here, the classic G_3 and G_4 codes [2] were employed as benchmarkers. Observe in Fig. 5 that each of the CSTSK schemes outperformed the corresponding STBC benchmarker, due to the CSTSK's capability of striking a flexible rate-diversity tradeoff. We note that each CSTSK arrangement was designed for the relation of $M > T$, rather than for $M = T$, where we aimed for an enhanced transmission rate, at the cost of sacrificing the full diversity order.

Next, we investigated the achievable BER performance of our DSTSK scheme in Fig. 6, where we considered a 4–PAM assisted DSTSK$(2, 2, 2, 4)$ system, achieving a normalized throughput of $R = 2.0$ bits/symbol. Here, we also plotted the BER curves of the SM schemes suffering from different levels of CSI estimation errors, where the estimated channels were contaminated by the additive Gaussian noise of $\mathcal{CN}(0, \omega)$ having a power of 5, 10 and 15 dB below the signal power, yielding equivalent SNRs of $\omega = -5$ dB, -10 dB and -15 dB. Furthermore, we employed the DLDC scheme of [4] as another benchmarker, where the MMSE criterion

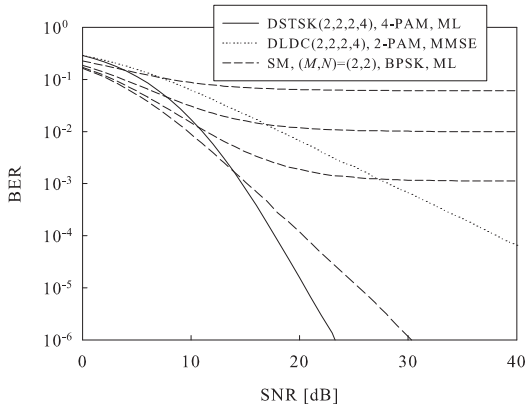

Fig. 6. Achievable BER curve of our DSTSK scheme, compared with the DLDC scheme as well as the SM scheme suffering from the CSI estimation error.

was employed for the DLDC's detection algorithm. Observe in Fig. 6 that as expected, our DSTSK scheme achieved a diversity order of four, hence outperforming both the DLDC scheme and the coherent SM scheme, which suffered from CSI estimation errors. Additionally, even for the case of no CSI error, the BER performance of our DSTSK scheme was better than that of the coherent SM scheme.

VI. Conclusions

In this paper we proposed coherent and differential STSK modulation schemes based on the novel concept of the dispersion matrix activation, which enables us to strike the required tradeoff between the MIMO's diversity and multiplexing gains, while maintaining a low decoding complexity owing to the resultant ICI-free system model obtained. The proposed STSK schemes may be viewed as the family of unified shift keying arrangements, including the recently-proposed SM and SSK schemes as their special cases. We also extended the CSTSK scheme to insure that no IAS is required between the RF branches associated with the transmit AEs.

The proposed STSK concept will also be applied to cooperative MIMO techniques [9].

References

[1] P. Wolniansky, G. Foschini, G. Golden, and R. Valenzuela, "V-BLAST: An architecture for realizing very high data rates over the rich-scattering wireless channel," in *Proceedings of the International Symposium on Signals, Systems, and Electronics*, Pisa, Italy, 1998, pp. 295–300.

[2] V. Tarokh, N. Seshadri, and A. Calderbank, "Space-time codes for high data rate wireless communication: performance criterion and code construction," *IEEE Transactions on Information Theory*, vol. 44, no. 2, pp. 744–765, 1998.

[3] B. Hassibi and B. Hochwald, "High-rate codes that are linear in space and time," *IEEE Transactions on Information Theory*, vol. 48, no. 7, pp. 1804–1824, 2002.

[4] ——, "Cayley differential unitary space-time codes," *IEEE Transactions on Information Theory*, vol. 48, no. 6, pp. 1485–1503, 2002.

[5] R. Mesleh, H. Haas, S. Sinanovic, C. Ahn, and S. Yun, "Spatial modulation," *IEEE Transactions on Vehicular Technology*, vol. 57, no. 4, pp. 2228–2242, 2008.

[6] J. Jeganathan, A. Ghrayeb, and L. Szczecinski, "Spatial modulation: optimal detection and performance analysis," *IEEE Communications Letters*, vol. 12, no. 8, pp. 545–547, 2008.

[7] J. Jeganathan, A. Ghrayeb, L. Szczecinski, and A. Ceron, "Space shift keying modulation for MIMO channels," *IEEE Transactions on Wireless Communications*, vol. 8, no. 7, pp. 3692–3703, 2009.

[8] L. Hanzo, O. Alamri, M. El-Hajjar, and N. Wu, *Near-Capacity Multi-Functional MIMO Systems: Sphere-Packing, Iterative Detection and Co-operation*. John Wiley and IEEE Press, 2009, **714 pages**.

[9] S. Sugiura, S. Chen, and L. Hanzo, "Packet-reliability based decode-and-forward relaying aided distributed space-time shift keying," in *IEEE Global Telecommunications Conference*, Miami, Florida, USA, 6–10 December 2010.